



Research paper

Study on temperature characteristics of multi-tower cable-stayed bridge

Liu Chengyuan¹, Han Zhuowei², Li Wei³, Zhao Lin⁴

Abstract: Temperature effects have a great influence on the mechanical behavior of cable-stayed bridges, especially for long-span bridges, which have significant time-varying and spatial effects. In this paper, the temperature characteristics of multi-tower cable-stayed bridge are obtained by data acquisition with wireless acquisition module. The test results show that: the daily temperature-time curves of atmospheric temperature and structural temperature are similar to sine waves with obvious peaks and troughs; structure temperature and atmospheric temperature have obvious hysteresis; longitudinal displacement, transverse displacement and vertical of mid-span beam are negatively correlated with atmospheric temperature; the temperature distribution of the cable tower is not uniform, and the maximum temperature difference of the section is 23.7°C considering 98% of the upper limit value; the longitudinal, transverse and vertical displacement of cable tower and the cable force is negatively correlated with atmospheric temperature, and the relationship between cable force and atmospheric temperature is a cubic function rather than linear function.

Keywords: atmospheric temperature, cable-stayed bridge, cable force, structure displacement

¹M.Eng., Shandong High-speed Group Co., Ltd., No. 0, Longding Road, Jinan, China, e-mail: liuchengyuansd@163.com, ORCID: 0009-0004-3133-967X

²M.Eng., Graduate student, Geotechnical and Structural Engineering Research Center, Shandong University, Jinan 250061, PR China, e-mail: 249192408@qq.com, ORCID: 0000-0002-6072-2887

³M.Eng., Shandong Expressway Jinan West Ring Road Co., Ltd, No. 15551, Jingshi Road, Jinan, China, e-mail: liweisd321@163.com, ORCID: 0009-0003-1565-7339

⁴M.Eng., Shandong Expressway Jinan West Ring Road Co., Ltd, No. 15551, Jingshi Road, Jinan, China, e-mail: liweisd321@zhaolinsd321@163.com, ORCID: 0009-0008-1338-8960

1. Introduction

Bridge structures are inevitably affected by various natural environmental factors [1]. The change of solar radiation and atmospheric temperature will cause the temperature of internal structure changed, resulting in a large non-uniform temperature gradient and considerable temperature stress in bridge structure [2, 3]. It is significant to study the influence of temperature change on bridge characteristics.

Finite element analysis and field monitoring are the main methods to study the temperature effect of bridge structures [4–6]. Lee et al. [7] carried out a long-term experimental and analysis research on prestressed concrete beam segments, evaluated the transverse temperature gradient which are not provided in AASHTO specifications, and proposed a second-order curve. Xia et al. [8] established the finite element model of Tsing Ma Bridge, by comparing the field monitoring data with the numerical calculation results, the accurate temperature distribution and associated responses of the bridge structure were obtained. Xu et al. [9] based on numerical simulation, analyzed the influence of temperature effects on the dynamic characteristics of bridge, pointed out that, for dynamic characteristics of bridge, the influence of temperature changes may greater than damage in girders or cables. Kuryowic et al. [10] considered laboratory tests, field measurements and numerical calculations for all research stages of bridge construction, established a maturity method to predict the temperature distribution of bridge structure. Liu et al. [11] based on a long-term bridge temperature monitoring database, proposed two positive vertical temperature gradient profiles and one negative vertical temperature gradient profile.

The temperature characteristics of different bridge structures are not consistent. Yang et al. [12] based on temperature monitoring and displacement data, studied the temperature field distribution of steel girder cable-stayed bridge and analyzed the relationship between tower displacement and temperature variation. As the stiffness of concrete girder cable-stayed bridge is significantly higher than steel girder cable-stayed bridge, the sensitivity of these two types of bridges to temperature variation is different [13, 14]. Some related researches indicate that the bridge monitoring model based on data-driven model can accurately evaluate the environmental impact of bridges [15–17]. Different from previous evaluation method of bridge environmental impact based on modified finite element model, the method based on data-driven model will be more direct and effective. Currently, there are few studies on temperature characteristics of multi-tower concrete girder cable-stayed bridge. This paper based on a large number of temperature monitoring data of bridge, established a data-driven model of bridge temperature, analyzed the influence of temperature variation on cable tower displacement and cable force.

2. Bridge structure and monitoring system

2.1. Monitoring system

Based on the analysis of monitoring data of Bridge, the thermal field characteristics, time variability of structural quasi-static displacement and the correlation between struc-

tural temperature and displacement are studied. The monitoring items mainly include five parts, temperature, wind speed, solar radiation, structural deformation and cable force. All measured data are collected and saved by automatic test system.

2.1.1. Environmental factor monitoring

JMT-36C thermistor temperature sensor is used in the bridge, which has the advantages of high accuracy, high stability, high reliability, moisture resistance and good insulation. It can accurately measure the temperature value inside the concrete structure. Wind speed, wind direction and solar radiation are collected by JMFY-1F wind speed and direction sensor and JMFY-1G solar radiation sensor. The sensor is made of metal and has strong anti-interference ability. It has the advantages of fast acquisition speed and good long-term stability, suitable for long-term monitoring. All the environmental monitoring equipment is shown in Fig. 1.

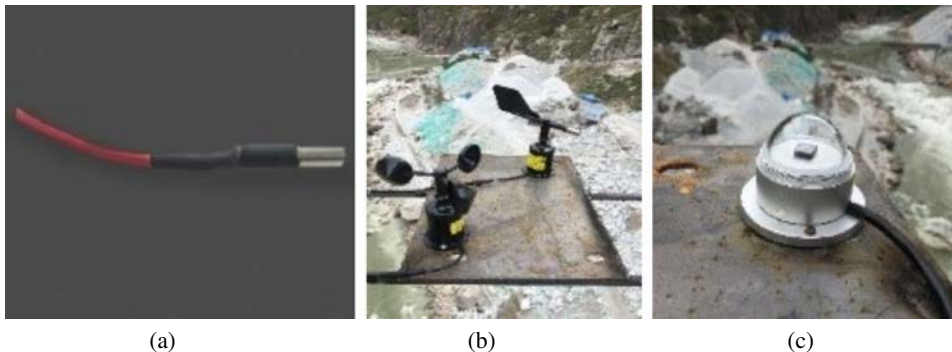


Fig. 1. Environmental monitoring equipment: a) temperature test instrument, b) wind speed test instrument, c) solar radiation test instrument

In order to obtain a more comprehensive temperature field distribution of the cable-stayed bridge, a total of 100 temperature sensors are arranged to monitor the temperature of the cable tower and girder.

2.1.2. Cable force monitoring

The variation method is used to measure the cable force by measuring the variation frequency of the cable. The acceleration sensors is fixed on the cable with special fixture to measure the variation of the cable and transforms the random variation signal into electrical signal, which is amplified by amplifier and sent to FFT signal analyzer for spectrum analysis to obtain the lateral variation frequency of the cable, by analyzing, the cable force is obtained, subsequently.

A total of 9 acceleration sensors are arranged to monitor the cable force of cables in real-time dynamic monitoring. The cable force monitoring equipment is shown in Fig. 2.

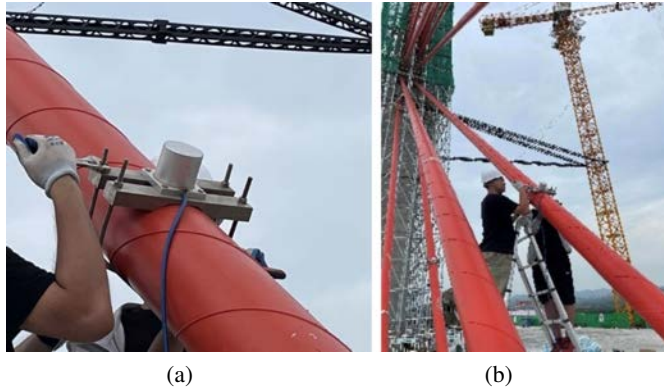


Fig. 2. Cable force monitoring equipment: a) acceleration sensors, b) field arrangement

2.1.3. Displacement monitoring

The bridge displacement monitoring equipment adopted JMBD-1050 Beidou remote displacement acquisition module, which can accurately measure the three-dimensional displacement value of a point on the bridge. A total of 4 displacement monitoring points are arranged along the longitudinal of the bridge.

3. Temperature characteristics of mid-span beam

3.1. Correlation between girder temperature and atmospheric temperature

Compared with atmospheric temperature, structure temperature is the critical factor which caused structure response, so it is necessary to analyze the correlation between structure temperature and atmospheric temperature. The temperature-time curve is shown in Fig. 3.

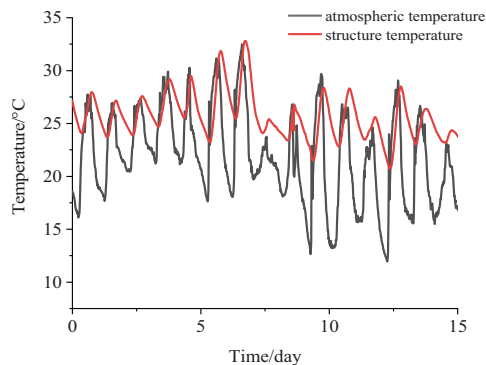


Fig. 3. Monthly atmospheric temperature and structural temperature of mid-span beam

As shown in Fig. 4. The upper limit of atmospheric temperature and structure temperature are almost consistent, while the lower limit of structural temperature is significantly higher than the lower limit of atmospheric temperature. There is a large difference between atmospheric temperature and structural temperature. In order to study the daily variation of atmospheric temperature and structure temperature, the monitoring data were analyzed.

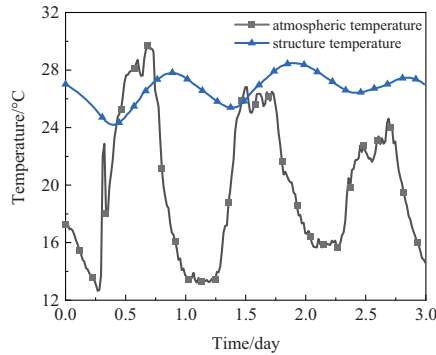


Fig. 4. Daily atmospheric temperature and structural temperature of mid-span beam

It can be seen from Fig. 4 that the daily temperature-time curves of atmospheric temperature and structural temperature are similar to sine waves, with obvious peaks and troughs. Compared with the atmospheric temperature, the structural temperature has obvious hysteresis.

3.2. Correlation between girder displacement and atmospheric temperature

The longitudinal and transverse displacement obtained by GPS are not the actual displacement of the bridge. The positive direction of the displacement measured by GPS is as follows: the longitudinal displacement is positive in the east, the transverse displacement is positive in the north and the vertical is positive in the upward direction, so the actual displacement of the bridge can be calculated by Eq. (3.1) and (3.2).

$$(3.1) \quad X'_{WE} = X_{WE} \cos 20^\circ + Y_{NS} \sin 20^\circ$$

$$(3.2) \quad Y'_{NS} = X_{WE} \sin 20^\circ - Y_{NS} \cos 20^\circ$$

where: X_{WE} – displacement in the east-west direction measured by GPS, X'_{WE} – displacement of the actual bridge in the east-west direction, Y_{NS} – displacement in the north-south direction measured by GPS, Y'_{NS} – displacement of the actual bridge in the east-west direction.

A total of 3 measuring points are arranged for monitoring the displacement of the mid-span beam. The correlation between bridge displacement and atmospheric temperature is analyzed by the monitoring data. Fig. 5 shows the correlation between three-dimensional displacement of the bridge and atmospheric temperature.

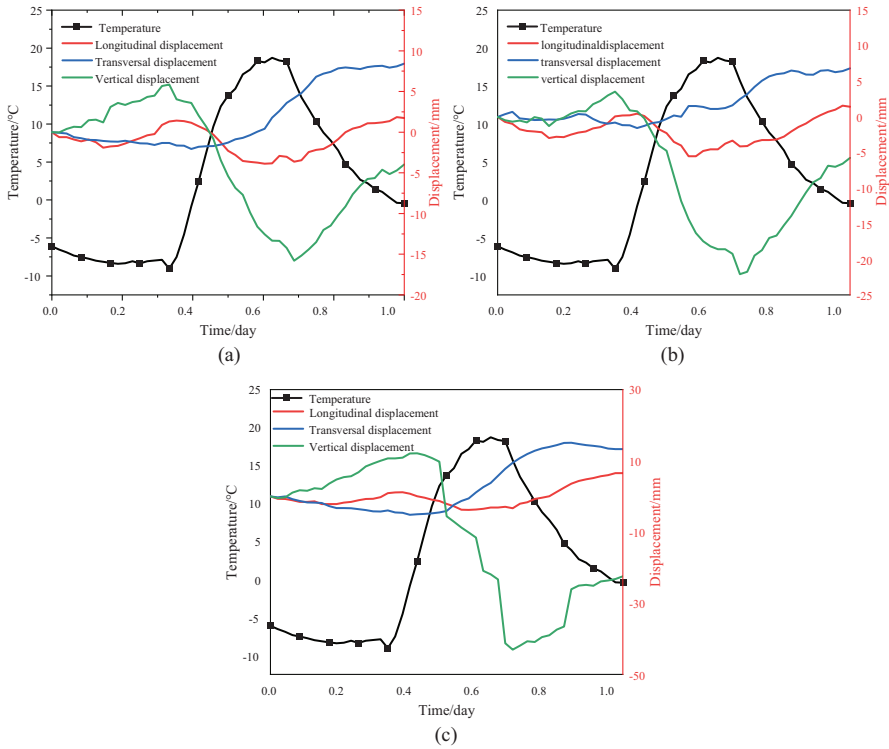
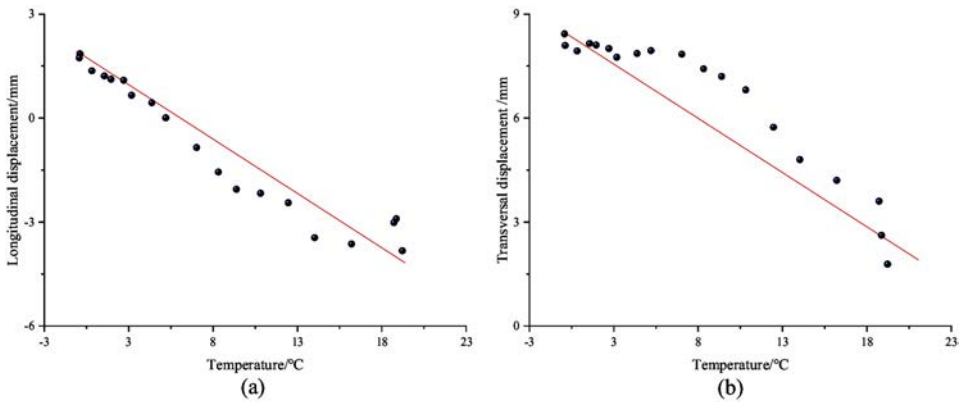


Fig. 5. Correlation between displacement and atmospheric temperature of mid-span beam. Measuring point: a) 1, b) 2, c) 3

Taking measuring point 1 as an example. It can be seen from Fig. 6. that the longitudinal, transversal and vertical displacement of the bridge are negatively correlated with atmospheric temperature, and the correlation coefficient R^2 are 0.87, 0.89 and 0.86, respec-



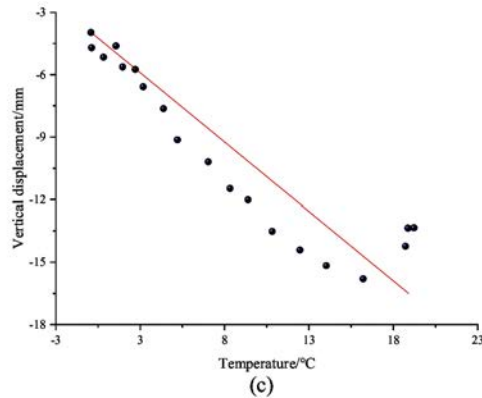


Fig. 6. Three-dimensional displacement-temperature curve of measuring point 1. a) longitudinal displacement, b) transversal displacement, c) vertical displacement

tively. It shows that with the increase of temperature, the three-dimensional displacement of the bridge will decrease.

4. Temperature characteristics of cable tower

4.1. Correlation between tower temperature and atmospheric temperature

The monitoring positions of cable tower temperature are at the same height. Three measuring points are arranged on each side and a total of 12 measuring points are arranged. The distributions of daily maximum temperature, minimum temperature and maximum temperature difference for each side are shown in Fig. 7.

As can be seen from Fig. 7, due to direct sunlight, the highest temperature side of the cable tower appears to the south side (sunny side). Since all measuring points are at the same height, the convection speed on all sides of the cable tower are identical. Except for the north side (back side), the temperature of the cable tower varied greatly in a single day. Take the three days with the largest temperature difference in a single day as an example, the temperature-time curve of each measuring point are plotted.

It can be seen from Fig. 8 that the temperature variation trend of each measuring point of the tower is different. Since the east side of the tower is exposed to solar radiation earlier, the temperature peak appears first, while the west side of the tower is exposed to solar radiation later, with the peak occurring around 4 p.m.

As shown in Fig. 9, The maximum temperature variation of the tower follows the Weibull distribution with parameter W (1.61, 10.14). The recurrence period of representative value of temperature effect is 50 years, and the design reference period of bridge specified in the General Code for Design Highway Bridges and Culverts (JTG D60-2015)

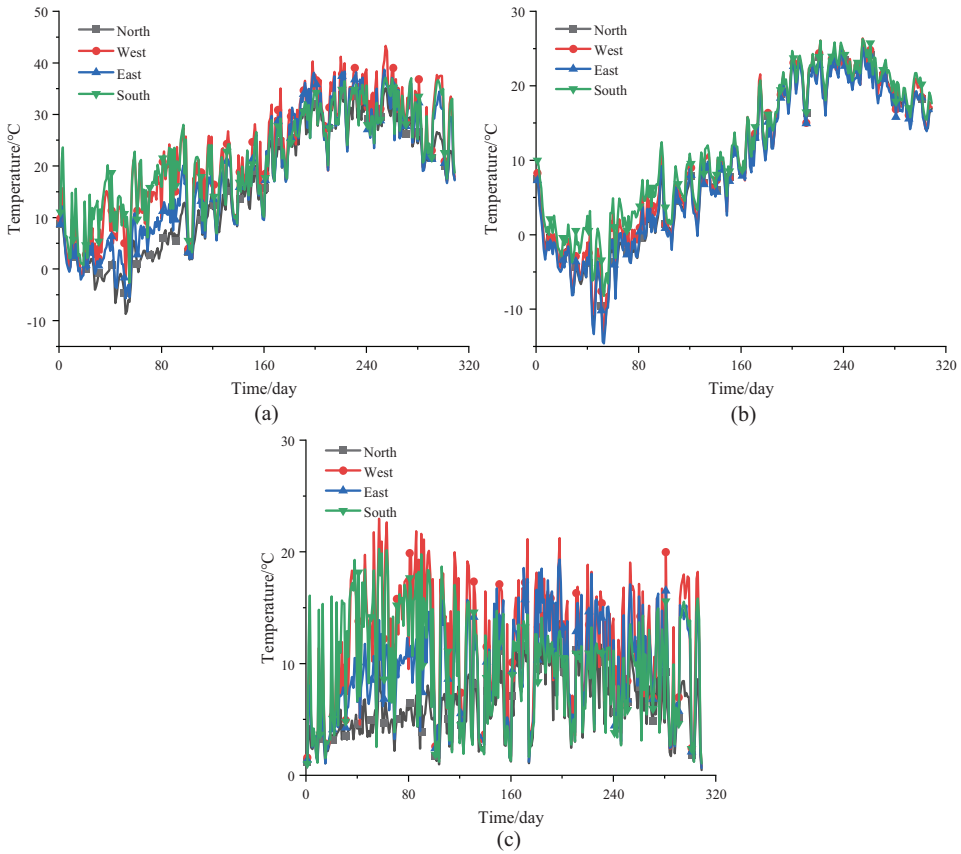


Fig. 7. Temperature distribution of cable tower: a) daily maximum temperature, b) daily minimum temperature, c) daily maximum temperature difference

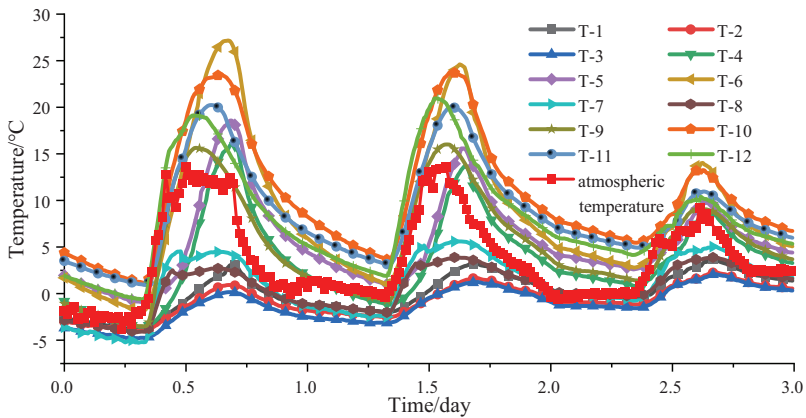


Fig. 8. Temperature-time curve of cable tower

of China [18] is 100 years. The number of times that the representative value of temperature effect is exceeded in the design reference period is 2, and the probability of exceeding is 98%, from which the maximum temperature variation was calculated to be 23.7°C.

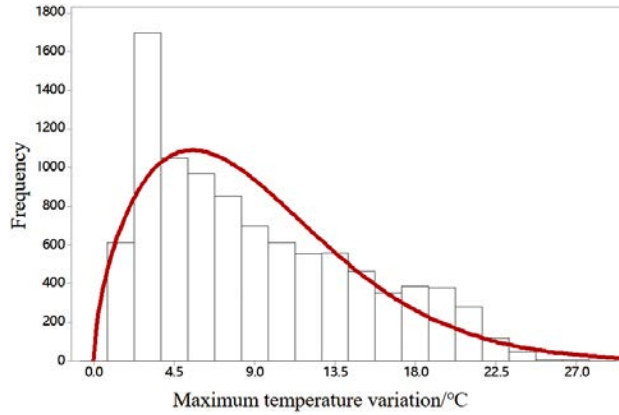
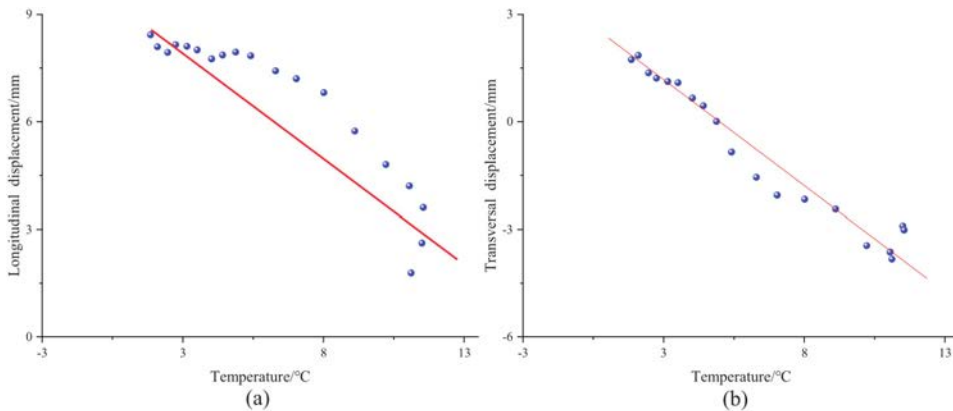


Fig. 9. Maximum temperature variation distribution of cable tower

4.2. Correlation between tower displacement and atmospheric temperature

The actual displacement of the cable tower can be calculated according to Eq. (3.1) and Eq. (3.2). In order to display the relationship between tower displacement and temperature more intuitively, the monitoring data which has the largest variation in atmospheric temperature during the test is selected to statistical analysis. As can be seen from Fig. 10, the longitudinal, transverse and vertical displacement of the tower are negatively correlated with temperature, and the correlation coefficient R^2 are 0.84, 0.89 and 0.86, respectively.



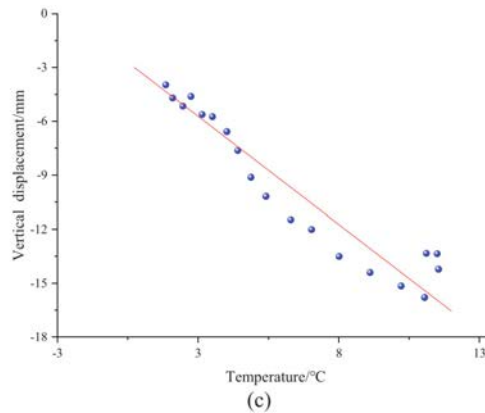


Fig. 10. Correlation between displacement and temperature of cable tower: a) longitudinal displacement, b) transversal displacement, c) vertical displacement

5. Temperature characteristics of stay cables

5.1. Testing principle of cable force

The cable force can be calculated according to Eq. (5.1) and Eq. (5.2).

$$(5.1) \quad T = KF^2$$

$$(5.2) \quad K = 4WL^2/1000$$

where: T – tensile force of stay cable, K – proportional coefficient, which calibrated by the test, F – basic frequency of stay cable, W – mass of unit length of stay cable, L – length between two embedded points of stay cable.

The parameters of the stay cable are shown in Table 1.

Table 1. Parameters of the stay cable

Cable number	Linear density (kg/m)	Length (m)	Working length (m)
1	47.343	45.768	43.768
2	47.343	49.915	47.915
4	47.343	58.208	56.208
6	47.343	66.501	64.501
8	47.343	74.793	72.793
10	47.343	83.084	81.084
12	47.343	91.376	89.376
14	47.343	99.671	97.671
15	47.343	101.818	101.818

5.2. Correlation between cable force and atmospheric temperature

It can be seen from Fig. 11 that all cable forces are negatively correlated with temperature, and with the increase of temperature, the cable force will descend. Due to the obvious fluctuation of cable force monitoring data, Savitzky-Golay filter [19] is used to smooth the data, that is, to improve the accuracy of the data without changing the signal trend. The data processed by the filter can be fitted by Eq. (5.3).

$$(5.3) \quad T = at^3 + bt + c$$

where: T – tensile force of stay cable, t – atmospheric temperature, a , b , c – fitting coefficient.

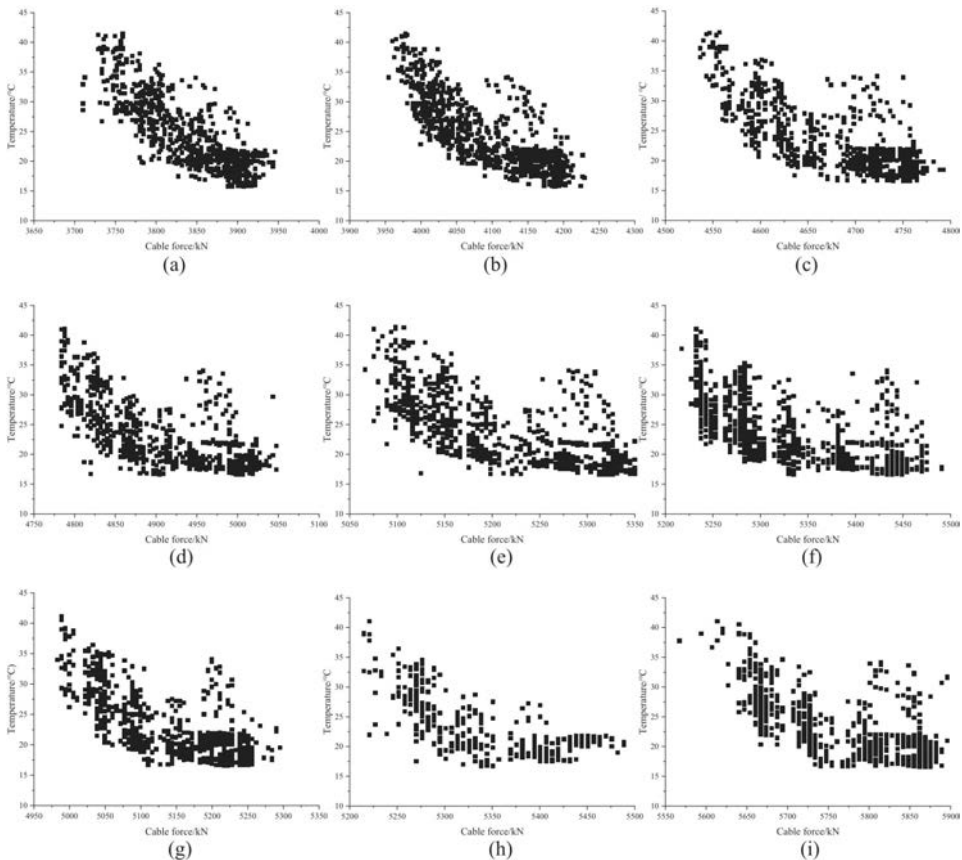


Fig. 11. Correlation between temperature and cable force.
 Cable: a) 1, b) 2, c) 4, d) 6, e) 8, f) 10, g) 12, h) 14, i) 15

The values of parameter a , b , c and correlation coefficient R^2 of each test cable are shown in Table 2.

Table 2. Parameter values of Eq. (5.3)

Parameter	Cable 1	Cable 2	Cable 4	Cable 6	Cable 8	Cable 10	Cable 12	Cable 14	Cable 15
a	3451.90	4475.74	4976.83	5277.29	5661.35	5740.13	5502.58	5640.69	6159.70
b	-15.94	-18.05	-14.16	-18.66	-22.66	-20.61	-17.61	-13.64	-19.52
c	0.005	0.004	0.002	0.004	0.006	0.006	0.003	0.002	0.004
R^2	0.94	0.93	0.88	0.86	0.88	0.85	0.89	0.77	0.86

According to Eq. (5.3) and Table 2, the comparison curves of theoretical and measured values of each cable force are plotted in Fig. 12. It can be seen that Eq. (5.3) can accurately predict the cable force. With the increase of temperature, the cable force gradually descend, and the relationship between cable force and atmospheric temperature is a cubic function rather than a linear function.

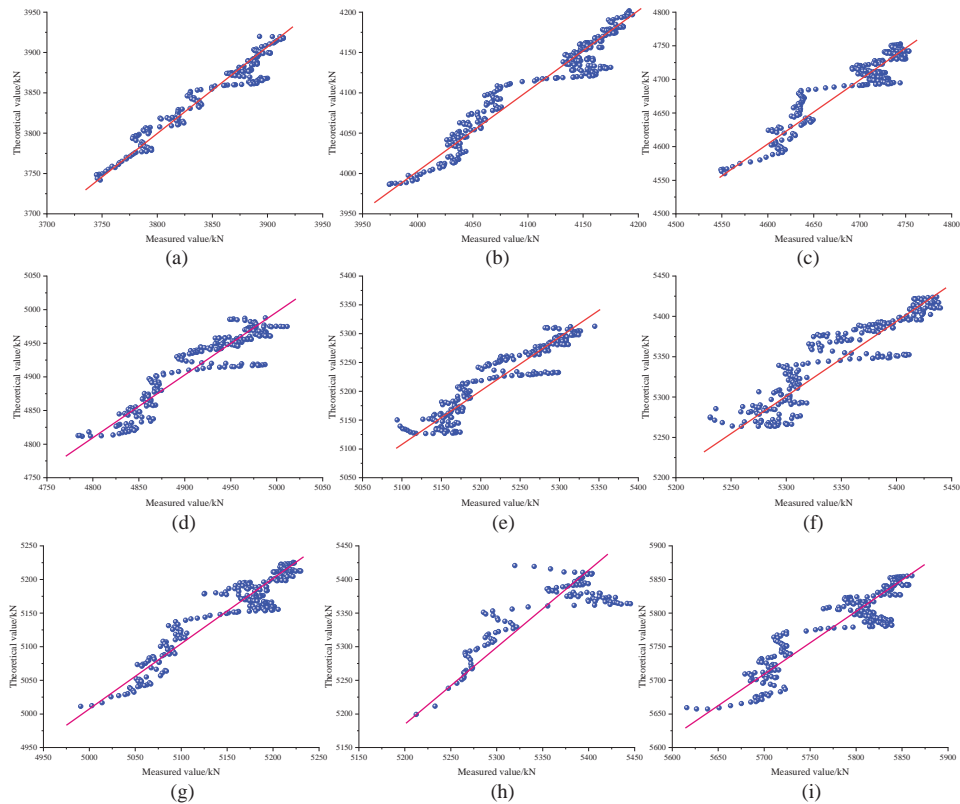


Fig. 12. Correlation between measured value and theoretical value of cable force.
 Cable: a) 1, b) 2, c) 4, d) 6, e) 8, f) 10, g) 12, h) 14, i) 15

6. Conclusions

In this paper, the temperature characteristics of multi-tower cable-stayed bridge is studied:

1. The longitudinal, transverse and vertical displacement of the mid-span beam are negatively correlated with atmospheric temperature. With the increase of temperature, the three-dimensional displacement of the bridge will decrease, and the correlation coefficient R^2 are 0.87, 0.89 and 0.86, respectively.
2. The temperature distribution of the cable tower is not uniform. The temperature on the sunny side changes significantly, the daily temperature variation can reach to 29.1°C, while the temperature on the back side changes slightly. The maximum temperature difference of the section considering 98% upper limit value is 23.7°C.
3. The longitudinal, transverse and vertical displacement of the cable tower are negatively correlated with temperature. With the increase of temperature, the three-dimensional displacement of the tower will decrease.
4. The cable force is negatively correlated with atmospheric temperature, and the relationship between cable force and atmospheric temperature is a cubic function rather than a linear function.

References

- [1] M.P. Collins and D. Mitchell, *Prestressed concrete structures*. Prentice Hall Englewood Cliffs, NJ, 1991.
- [2] L. Krkoska and M. Moravcik, "Monitoring of temperature gradient development of highway concrete bridge", *MATEC Web of Conferences*, vol. 117, art. no. 00091, 2017, doi: [10.1051/mateconf/201711700091](https://doi.org/10.1051/mateconf/201711700091).
- [3] R. Westgate, K.Y. Koo, and J. Brownjohn, "Effect of Solar Radiation on Suspension Bridge Performance", *Journal of Bridge Engineering*, vol. 20, no. 5, 2014, doi: [10.1061/\(ASCE\)BE.1943-5592.0000668](https://doi.org/10.1061/(ASCE)BE.1943-5592.0000668).
- [4] E. Mirambell and A. Aguado, "Temperature and Stress Distributions in Concrete Box Girder Bridges", *Journal of Structural Engineering*, vol. 116, no. 9, pp. 2388–2409, 1990, doi: [10.1061/\(ASCE\)0733-9445\(1990\)116:9\(2388\)](https://doi.org/10.1061/(ASCE)0733-9445(1990)116:9(2388)).
- [5] N. Taysi and S. Abid, "Temperature Distributions and Variations in Concrete Box-Girder Bridges: Experimental and Finite Element Parametric Studies", *Advances in Structural Engineering*, vol. 18, no. 4, pp. 469–486, 2015, doi: [10.1260/1369-4332.18.4.469](https://doi.org/10.1260/1369-4332.18.4.469).
- [6] Y.H. Cao, J. Yim, Y. Zhao, and M.L. Wang, "Temperature effects on cable stayed bridge using health monitoring system: a case study", *Structural Health Monitoring*, vol. 10, no. 5, pp. 523–537, 2011, doi: [10.1177/1475921710388970](https://doi.org/10.1177/1475921710388970).
- [7] J.H. Lee and I. Kalkan, "Analysis of thermal environmental effects on precast, prestressed concrete bridge girders: temperature differentials and thermal deformations", *Advances in Structural Engineering*, vol. 15, no. 3, pp. 447–459, 2012, doi: [10.1260/1369-4332.15.3.447](https://doi.org/10.1260/1369-4332.15.3.447).
- [8] Y. Xia, B. Chen, X.Q. Zhou, and Y.L. Xu, "Field monitoring and numerical analysis of Tsing Ma Suspension Bridge temperature behavior", *Structural Control & Health Monitoring*, vol. 20, no. 4, pp. 560–575, 2013, doi: [10.1002/stc.515](https://doi.org/10.1002/stc.515).
- [9] Z.D. Xu and Z. Wu, "Simulation of the effect of temperature variation on damage detection in a long-span cable-stayed bridge", *Structural Health Monitoring*, vol. 6, no. 3, pp. 177–189, 2007, doi: [10.1177/1475921707081107](https://doi.org/10.1177/1475921707081107).
- [10] A. Kuryłowicz-Cudowska, K. Wilde, and J. Chróścielewski, "Prediction of cast-in-place concrete strength of the extradosed bridge deck based on temperature monitoring and numerical simulations", *Construction and Building Materials*, vol. 254, art. no. 119224, 2020, doi: [10.1016/j.conbuildmat.2020.119224](https://doi.org/10.1016/j.conbuildmat.2020.119224).

- [11] J. Liu, Y. Liu, L. Jiang, and N. Zhang, “Long-term field test of temperature gradients on the composite girder of a long-span cable-stayed bridge”, *Advances in Structural Engineering*, vol. 22, no. 13, pp. 2785–2798, 2019, doi: [10.1177/1369433219851300](https://doi.org/10.1177/1369433219851300).
- [12] D.H. Yang, T.H. Yi, H.N. Li, and Y.F. Zhang, “Monitoring and analysis of thermal effect on tower displacement in cable-stayed bridge”, *Measurement*, vol. 115, pp. 249–257, 2018, doi: [10.1016/j.measurement.2017.10.036](https://doi.org/10.1016/j.measurement.2017.10.036).
- [13] S.H. Kim, S.J. Park, J.X. Wu, and J.H. Won, “Temperature variation in steel box girders of cable-stayed bridges during construction”, *Journal of Constructional Steel Research*, vol. 112, pp. 80–92, 2015, doi: [10.1016/j.jcsr.2015.04.016](https://doi.org/10.1016/j.jcsr.2015.04.016).
- [14] O. Larsson and S. Thelandersson, “Estimating extreme values of thermal gradients in concrete structures”, *Materials and Structures*, vol. 44, pp. 1491–1500, 2011, doi: [10.1617/s11527-011-9714-0](https://doi.org/10.1617/s11527-011-9714-0).
- [15] J.X. Mao, H. Wang, D.M. Feng, T.Y. Tao, and W.Z. Zheng, “Investigation of dynamic properties of long-span cable-stayed bridges based on one-year monitoring data under normal operating condition”, *Structural Control and Health Monitoring*, vol. 25, no. 5, pp. 1–19, 2018, doi: [10.1002/stc.2146](https://doi.org/10.1002/stc.2146).
- [16] Y.M. Zhang, H. Wang, Y. Bai, J.X. Mao, X.Y. Chang, and L.B. Wang, “Switching Bayesian dynamic linear model for condition assessment of bridge expansion joints using structural health monitoring data”, *Mechanical Systems and Signal Processing*, vol. 160, art. no. 107879, 2021, doi: [10.1016/j.ymsp.2021.107879](https://doi.org/10.1016/j.ymsp.2021.107879).
- [17] Y.M. Zhang, H. Wang, H.P. Wan, J.X. Mao, and Y.C. Xu, “Anomaly detection of structural health monitoring data using the maximum likelihood estimation-based Bayesian dynamic linear model”, *Structural Health Monitoring*, vol. 20, no. 6, pp. 2936–2952, 2021, doi: [10.1177/1475921720977020](https://doi.org/10.1177/1475921720977020).
- [18] JTG D60-2015 General Code for Design Highway Bridges and Culverts. Ministry of Transport of the People’s Republic of China, 2015.
- [19] W.H. Press, B.P. Flannery, S.A. Teukolsky, and W.T. Vetterling, “Savitzky-Golay Smoothing Filters”, *Computers in Physics*, vol. 4, pp. 669–672, 1990, doi: [10.1063/1.4822961](https://doi.org/10.1063/1.4822961).

Received: 2023-03-08, Revised: 2023-08-29